



You have downloaded a document from  
**RE-BUŚ**  
repository of the University of Silesia in Katowice

**Title:** Characteristics of natural background radiation in the GIG Experimental Mine 'Barbara', Poland

**Author:** Agata Walencik-Łata, Katarzyna Szkliniarz, Jan Kisiel [i in.]








**Citation style:** Walencik-Łata Agata, Szkliniarz Katarzyna, Kisiel Jan [i in.]. (2022). Characteristics of natural background radiation in the GIG Experimental Mine 'Barbara', Poland. „Energies (Basel)” (Vol. 15, iss. 3, 2022, art. no. 685, s. 1-12), DOI: 10.3390/en15030685



Uznanie autorstwa - Licencja ta pozwala na kopiowanie, zmienianie, rozprowadzanie, przedstawianie i wykonywanie utworu jedynie pod warunkiem oznaczenia autorstwa.

## Article

# Characteristics of Natural Background Radiation in the GIG Experimental Mine ‘Barbara’, Poland

Agata Walencik-Łata <sup>1,\*</sup>, Katarzyna Szkliniarz <sup>1</sup>, Jan Kisiel <sup>1</sup>, Kinga Polaczek-Grelík <sup>2</sup>, Karol Jędrzejczak <sup>3</sup>, Marcin Kasztelan <sup>3</sup>, Jacek Szabelski <sup>3</sup>, Jerzy Orzechowski <sup>3</sup>, Przemysław Tokarski <sup>3</sup>, Włodzimierz Marszał <sup>3</sup>, Marika Przybylak <sup>3</sup>, Robert Hildebrandt <sup>4</sup> and Krzysztof Fuławka <sup>5</sup>

<sup>1</sup> August Chełkowski Institute of Physics, University of Silesia in Katowice, 75 Pułku Piechoty 1, 41-500 Chorzów, Poland; katarzyna.szkliniarz@us.edu.pl (K.S.); jan.kisiel@us.edu.pl (J.K.)

<sup>2</sup> NU-Med Cancer Diagnosis and Treatment Centre Katowice, Ceglana 35, 40-514 Katowice, Poland; kinga.grelík@gmail.com

<sup>3</sup> National Centre for Nuclear Research, 28 Pułku Strzelców Kaniowskich 69, 90-558 Łódź, Poland; karol.jedrzejczak@ncbj.gov.pl (K.J.); marcin.kasztelan@ncbj.gov.pl (M.K.); jacek.szabelski@ncbj.gov.pl (J.S.); jerzy.orzechowski@ncbj.gov.pl (J.O.); przemyslaw.tokarski@ncbj.gov.pl (P.T.); wlodzimierz.marszal@ncbj.gov.pl (W.M.); marika.przybylak@ncbj.gov.pl (M.P.)

<sup>4</sup> Department of Underground Research and Surface Maintenance, Central Mining Institute, Podleska 72, 43-190 Mikołów, Poland; rhildebrandt@gig.eu

<sup>5</sup> KGHM CUPRUM Research & Development Centre, Sikorskiego 2-8, 53-659 Wrocław, Poland; kfulawka@cuprum.wroc.pl

\* Correspondence: agata.walencik@us.edu.pl; Tel.: +48-32-3497739



**Citation:** Walencik-Łata, A.;

Szkliniarz, K.; Kisiel, J.;

Polaczek-Grelík, K.; Jędrzejczak, K.;

Kasztelan, M.; Szabelski, J.;

Orzechowski, J.; Tokarski, P.; Marszał,

W.; et al. Characteristics of Natural

Background Radiation in the GIG

Experimental Mine ‘Barbara’, Poland.

*Energies* **2022**, *15*, 685. [https://](https://doi.org/10.3390/en15030685)

[doi.org/10.3390/en15030685](https://doi.org/10.3390/en15030685)

Academic Editor: Nikolaos

Koukouzas

Received: 9 December 2021

Accepted: 15 January 2022

Published: 18 January 2022

**Publisher’s Note:** MDPI stays neutral with regard to jurisdictional claims in published maps and institutional affiliations.



**Copyright:** © 2022 by the authors. Licensee MDPI, Basel, Switzerland. This article is an open access article distributed under the terms and conditions of the Creative Commons Attribution (CC BY) license (<https://creativecommons.org/licenses/by/4.0/>).

**Abstract:** Underground locations can be used in various ways for scientific and economic purposes. One of the main factors influencing the safety level in the underground mine workings is natural radioactivity. The article presents research carried out on the natural radioactivity in shallow mine workings at the GIG Experimental Mine ‘Barbara’. The description of the natural radiation includes radon determination in the air, in situ gamma spectrometry, neutron flux measurements, and laboratory measurements of <sup>226,228</sup>Ra, <sup>40</sup>K, and <sup>234,238</sup>U isotopes using gamma and alpha spectrometry techniques. In the measurement chamber at the depth 46 m (122 m w.e.) in the sandstone layer, the photon flux registered at the 7–3150 keV energy range is equal to  $17.6 \pm 1.9 \text{ cm}^{-2}\text{s}^{-1}$ , the gamma-ray dose rate is  $0.200 \pm 0.029 \text{ } \mu\text{Sv/h}$ , and the thermal neutron flux is equal to  $(8.6 \pm 1.1) \times 10^{-6} \text{ cm}^{-2}\text{s}^{-1}$ . After closing the measurement chamber and turning off ventilation, a significant ingrowth of <sup>222</sup>Rn content was observed, reaching the value of  $4040 \pm 150 \text{ Bq/m}^3$ . An increased gamma-ray flux and thermal neutron flux were observed in the investigated location.

**Keywords:** natural radiation; underground locations; radioisotopes concentration

## 1. Introduction

Underground laboratories are places where more and more activities can be carried out that are not only scientific but also requiring constant temperature and humidity conditions (these are the characteristics of underground sites), e.g., for breeding plants, fungi, or insects. Old disused mines, subway tunnels, tunnels, and other underground locations are often converted into underground laboratories that serve the public. Deep underground laboratories, such as those in Gran Sasso or Modane (depth over 1000 m), are mainly used to research physics and astrophysics, e.g., to search for dark matter or neutrinoless double beta decay [1,2]. However, there are many readily available shallow and medium-depth underground laboratories that have been used for a long time to measure radioactivity in various types of samples (e.g., river sediment, water, soil, rock samples [3], <sup>39</sup>Ar-dating [4], <sup>14</sup>C-dating [5], neutron activation analysis [6], selection of low-level materials [7], and many others). However, such locations are often characterized by a much greater natural radiation background than deep locations. Therefore, special shields are constructed, among other

things, of concrete, steel, and lead, reducing the level of natural radiation background. An example is the shallow laboratory “Felsenkeller” in Dresden, located at a depth of 47 m, where such tests are carried out in two specially designed measuring chambers [3].

The sources of natural radioactivity are long-lived isotopes, radionuclides originating from the  $^{232}\text{Th}$ ,  $^{238}\text{U}$ , and  $^{235}\text{U}$  decay chains. In addition, the source of natural radiation on the Earth is cosmic rays and cosmogenic radionuclides formed under the interaction of cosmic rays with the components of the atmosphere. The source of radioactivity on Earth is also the so-called anthropogenic activities, including coal combustion, production, the use of phosphorus fertilizers, the mining industry, the storage of radioactive waste in repositories, testing of nuclear weapons, and nuclear power plants [8]. For underground locations, the sources of natural radioactivity are primarily radionuclides present in the rocks and noble gas radon. Earlier studies have shown [9] that materials used as building materials, e.g., concrete building, can significantly increase radiation background.

Natural radioactivity research was carried out in one of the underground laboratories of the Associated Organization, GIG Experimental Mine (EM) ‘Barbara’, participating in the BSUIN (Baltic Sea Underground Innovation Network), and EUL (Empowering Underground Laboratories Network Usage) projects financed by the Interreg Baltic Sea Region. The EM ‘Barbara’ mine is a unique place where extensive research on gas and dust explosions can be carried out. In addition, research can be provided in real conditions of new technologies, machines, and devices for underground work. This allows for research and service work in mining, firefighting, construction, civil defense, and many other areas. In EM ‘Barbara’ previously, no natural radioactivity measurements were carried out, except for monitoring measures covered by the mining law, which in each case showed values below the permitted levels. Therefore, this paper includes detailed characteristics of natural radioactivity in EM ‘Barbara’ in a blind chamber. The research consists of in situ gamma-ray spectrometry, measurements of thermal neutron flux, the radon concentration in the air, as well as laboratory analysis of the concentration of radium ( $^{226,228}\text{Ra}$ ), uranium ( $^{234,238}\text{U}$ ), and potassium ( $^{40}\text{K}$ ) isotopes in the collected rock samples (sandstone) using alpha and gamma spectrometry.

### *Site Geology*

The study of natural radioactivity was carried out at the Experimental Mine ‘Barbara’, Poland, which is located in the central part of the Upper Silesian Coal Basin ( $50^{\circ}10'46.926''$  N  $18^{\circ}55'54.216''$  E). The mine is a part of Central Mining Institute, which is a unit that undertakes research for the needs of mining and geology. At EM ‘Barbara’, the underground workings were modernized and adapted to an experimental testing site. At present, the underground infrastructure enables numerous types of innovative research and projects, which are predominantly orientated on effectiveness and safety in mining and on environmental protection.

The EM ‘Barbara’ area is located in the southern wing of the main anticline on the south of the Kłodnica fault. The Quaternary and Productive Carboniferous formations take part in the geological structure of the deposit. Quaternary formations are sand, gravel, and clay. In a major part of the deposit’s area, the thickness of the Quaternary varies from 4 to 6 m. In some places in the southern and northeastern parts, the Carboniferous top occurs directly under the layer of the soil. Productive Carboniferous is represented by the Orzeskie and Łaziska Beds. The Łaziska Beds are formed in the sandstone-conglomerate facies, among which only in some places are there thin inserts of shale. The Orzeskie Beds are formed of alternating fine and medium-grained sandstones, in places conglomerate and shales, among which there are numerous deposits of hard coal. The rock mass within the range of active mining workings is not tectonically disturbed. Figure 1 shows a stratigraphic profile of the mine.

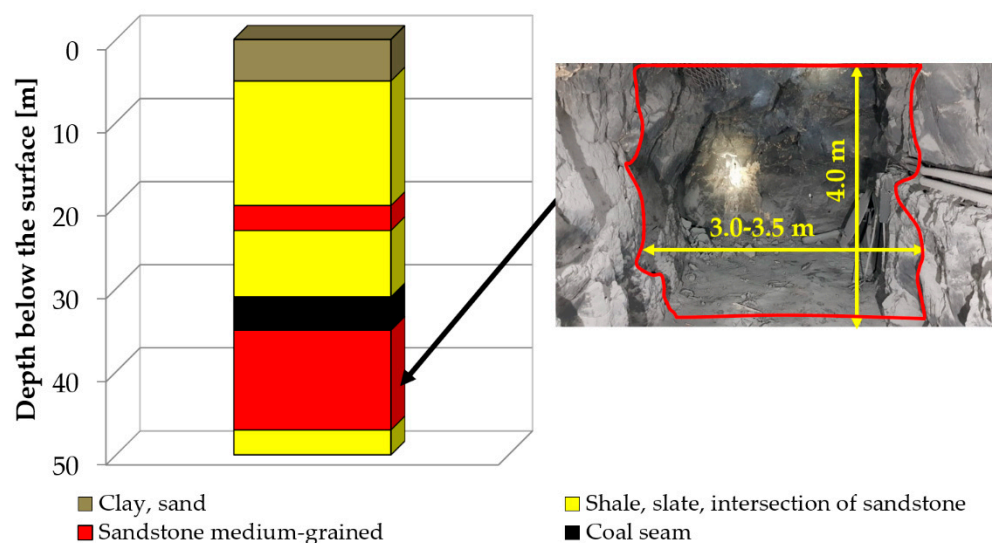


**Figure 1.** Stratigraphic profile of the GIG Experimental Mine ‘Barbara’.

## 2. Materials and Methods

Measurements of natural radioactivity in the EM ‘Barbara’ were carried out at the level of 46 m (122 m w.e.) in a 30 m × 3–3.5 m × 4 m indentation (Figure 1). The testing site was located at a blind chamber excavated in sandstone (Figure 2d). Sandstone’s parameters do not require the use of any additional support. The volume of the work was approximately 400 m<sup>3</sup>. The chamber walls where the measurements were made are bare sandstone, which is only supported by steel structural elements. The ventilation system and equipment in the workings surrounding the chamber allow its ventilation and airflow cut-off depending on the needs of tests. During normal working conditions, the mine ventilation provides the exchange of air in the area of the blind chamber between 50 and 100 m<sup>3</sup>/min. The testing site was characterized by stable air parameters with a temperature of 12 °C and humidity of 70%. A high-purity germanium (HPGe) semiconductor detector, RAD7 radon monitor, and helium neutron proportional counters were used for the measurements (Figure 2a–c). In order to perform a laboratory analysis in an external laboratory (at the A. Chełkowski Institute of Physics, the University of Silesia in Katowice, Poland), 18 rock samples were taken from the locations marked in Figure 2e. The representative samples were taken at intervals of 5 m (points marked from 1 to 18; see Figure 2e).

### 2.1. In Situ Gamma Spectrometry

In situ gamma radiation measurements in the EM ‘Barbara’ were performed using the same measurement system as during the measurements in the Polkowice-Sieroszowice mine [10]. The portable gamma spectrometer included a multichannel analyzer InInspector 2000, a high-purity germanium detector (HPGe), and software Gennie™ 2000 v.3.2.1. The detector used for the measurements has a carbon entry window with a thickness of 0.6 mm, a nominal efficiency of 40%, an FWHM of 2.1 keV at a 1.33 MeV <sup>60</sup>Co line, and a peak to Compton ratio 57/1, and it is cooled with liquid nitrogen. During the measurements, the detector was installed horizontally on a rack made of wood, 30 cm in front of the nearest wall (the center of the germanium crystal was 25 cm above the floor (Figure 2b)).

Energy calibration was performed using a set of sealed radioactive sources: <sup>133</sup>Ba, <sup>137</sup>Cs, <sup>54</sup>Mn, <sup>57</sup>Co, <sup>109</sup>Cd, <sup>22</sup>Na, and <sup>60</sup>Co, with a diameter of 1 cm and about 10 kBq activity. Efficiency calibration was done using ISOCS™ software (Canberra Industries, Inc., Meriden, CT, USA) for monoenergetic photons from the energy range of 10–3300 keV, which covers the useful measuring range of the spectrometer used in the in situ measurements. For this purpose, a room/box geometry with internal surface contamination was selected in the ISOCS™ software, which was modeled in the Geometry Composer software (Canberra Industries, Inc.). The photopeak efficiency ( $\epsilon$ ) calibration as a function of gamma-ray energy

(E) was fitted automatically in Gennie™ 2000 software to measurement geometry in the form of a 5th-order polynomial, as shown below (Equation (1)).

$$\ln(\epsilon) = -11.2 - 9.362\ln(E) + 6.135\ln(E)^2 - 1.447\ln(E)^3 + 0.1466\ln(E)^4 - 0.00547\ln(E)^5 \quad (1)$$

Gennie™ 2000 v.3.2.1 software was used to record and analyze the gamma-ray spectra registered in the 7–3150 keV energy range (for n-type HPGe detector used, with applying a total spectrometric gain of 5.0). Radioisotopes were identified in the spectra based on the photopeaks' energy. The area under each peak on the spectrum was determined using the automated analysis sequence involving unidentified second differential and non-linear Least Squares (LSQ) fit. Gamma-ray flux density was determined based on formula 2 presented previously in [10], taking into account the net area of each gamma line with the peak energy (E) in the recorded spectrum, the measurement lifetime (LT), detector area ( $S_{Ce}$ ), and detection efficiency ( $\epsilon$ ).

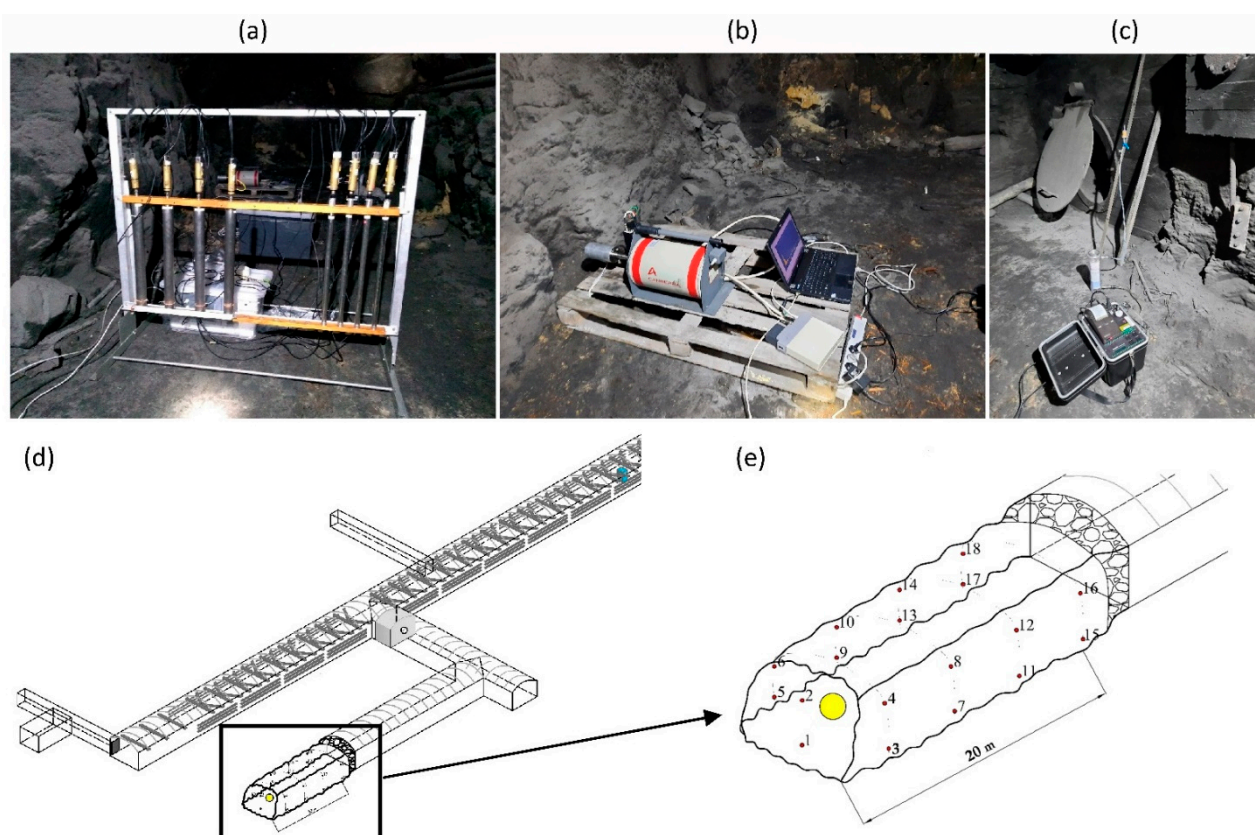


**Figure 2.** Measurement setup used during the measurements: (a) visible flat tray of helium counters placed vertically in the stand; (b) HPGe spectrometer; (c) RAD7 detector; (d) scheme of the workings where the research area was located; (e) enlarging the research area with the sampling site marked for laboratory analysis (the yellow dot marks the location of the measuring devices).

The effective dose at the spectrometer position during in situ measurements was determined using the photon flux to dose conversion factors from the ICRP report [11]. The uncertainties of the gamma-ray photon flux and the effective dose were estimated using the same methods as described in [10].

## 2.2. In Situ Radon Measurement in Air

The radon measurements in the air were performed using the RAD7 portable detector (DurrIDGE Company, Inc., Billerica, MA, USA). The  $^{222}\text{Rn}$  concentration in the air was obtained by using a 1-day protocol with a 0.5 h measurement cycle. This monitor was placed

next to the gamma spectrometer on the position marked in Figure 2e. The spectrometer uses a semiconductor Ion-implanted, Planar, Silicon detector to convert alpha particles to an electrical signal. In the Normal mode, the  $^{222}\text{Rn}$  concentration is determined based on measurements of alpha particles from daughter isotopes of  $^{214}\text{Po}$  and  $^{218}\text{Po}$ .

### 2.3. $\alpha$ and $\gamma$ Laboratory Spectrometry Techniques

The samples collected from 18 places (Figure 2e) were transferred to the laboratory. Then, samples were crushed, dried, and homogenized for alpha and gamma spectrometry measurements. Samples for gamma spectrometry measurements were placed in Marinelli beakers, tightly closed to avoid radon leakage, and left for one month to achieve radioactive equilibrium in thorium and uranium series.

Gamma radiation from samples was analyzed using a high-purity germanium (HPGe) detector (GC2018) of 60.7 mm crystal diameter and Cryo-Pulse 5 Plus, an electrically powered cryostat from Canberra-Packard. The detector has a relative efficiency of 20%, energy resolution (FWHM) of 1.7 keV, and Peak-to-Compton (P/C) ratio of 53.8:1 at 1.332 MeV gamma line from  $^{60}\text{Co}$ . The activities of  $^{226}\text{Ra}$ ,  $^{228}\text{Ra}$ , and  $^{40}\text{K}$  isotopes were calculated based on a standard prepared from certificated materials obtained from the Central Laboratory for Radiological Protection (CLOR) in Poland. The concentration of the  $^{40}\text{K}$  isotope was calculated from the 1460.8 keV gamma line. The concentrations of  $^{226}\text{Ra}$  and  $^{228}\text{Ra}$  isotopes were calculated as the weighted mean of the concentrations of daughter isotopes  $^{214}\text{Pb}$  (295.2, 351.9 keV),  $^{214}\text{Bi}$  (609.3, 1120.3 keV), and from  $^{228}\text{Ac}$  (338.3, 911.1 keV), respectively. Additionally, for six samples (sampling points 1–6 marked on Figure 2e) taken from places closest to the gamma and radon spectrometers, the laborious and time-consuming chemical preparation of samples for uranium isotope concentrations was performed. These samples placed in PTFE pressure decomposition vessels were digested using a microwave unit MAGNUM II (ERTEC-Poland). A standard of  $^{232}\text{U}$  isotope was added for each analyzed sample, and the wet mineralization was performed using hot acids: HF,  $\text{HNO}_3$ , and HCl with  $\text{H}_3\text{BO}_3$ . Uranium was pre-concentrated with iron and co-precipitated with ammonia at pH 9. Uranium isotopes were separated using the anion exchange resin Dowex 1  $\times$  8 ( $\text{Cl}^-$  type, 200–400 mesh). The alpha spectrometry source suitable for alpha spectrometry measurement was obtained from the co-precipitation of uranium fraction with  $\text{NdF}_3$  and filtration. The measurements of  $^{234,238}\text{U}$  isotopes were performed by using  $\alpha$  spectrometers 7401VR and Alpha Analyst<sup>TM</sup> (Mirion Technologies (Canberra), Inc., Meriden, CT, USA) equipped with passivated implanted planar silicon (PIPS) detectors. A detailed description of sample preparation may be found in [10,12]. The uncertainties of the activity concentrations for the above-mentioned isotopes were calculated using the same methods as presented in [10].

### 2.4. Neutron Flux Measurements

The same setup was used in the present study as in [10]. The thermal neutron flux measurements were performed using gas proportional counters filled with helium-3 ( $^3\text{He}$ ). The helium captures the nucleus in the reaction (Equation (2)):



and the charged products (proton and tritium) of the reaction have the sum of kinetic energies of 764 keV. Proton and tritium ionize and can be detected by a proportional counter, similar to standard radiation. This method is sensitive only for thermal neutrons with an energy of about 0.2 eV. The energy of these neutrons is negligible to the heat of the reaction (764 keV); hence, neutron registrations form a very characteristic “peak and tail” amplitude spectrum. This allows distinguishing neutrons events even with a large background of other types of radiation. The measurement setup consisted of a flat tray of helium counters positioned vertically in a rack Figure 2a. The tray was divided into two parts: first, there were four Centronic counters (Centronic 50He3/190/50MS), a 30 cm space, and again four ZDAJ counters (ZDAJ NEM425A50). There were 5 cm gaps between

the individual counters to limit a shadowing effect. The counters of both types were steel pipes 50 cm long, but they differed in diameter (5 cm for Centronic and 2.5 cm for ZDAJ) and helium-3 pressure (2 atm for Centronic and 4 atm for ZDAJ).

The data acquisition system (DAQ) was designed and made at the NCBJ laboratory in Łódź. DAQ is built in the form of a cassette with 8 measurement cards. Each card contains 4 independent measurement channels, up to 32 input channels in total. Each measurement channel is sampled with a frequency of 10 MHz by an ADC with a dynamic of 10 bits. A waveform is recorded after the trigger, with length dynamically adjusted to the current measured pulse length. For very short pulses (electronic disturbances), the run contained 32 samples. DAQ has flash memory and may work as an autonomous system without connecting to an external computer. The connection via the Internet was available during the measurements, and the setup work was monitored remotely. All recorded data were analyzed offline. As the measuring system recorded the pulses from counters, it was possible to analyze the pulse shape for each event. This is a key issue in determining the rate of counts. In underground laboratories, very few neutrons are usually recorded (a few counts per counter per hour), while the DAQ may be triggered by the number of background pulses interfering with the measurement. The pulse shape analysis was based on the two-dimensional distribution of the maximum pulse amplitude versus the maximum pulse step rise on the rising edge. In such a distribution, pulses of different shapes populate separate areas. Laboratory measurements approved that method for separating neutron-induced pulses from others.

To determine the neutron flux, it is necessary to use Monte Carlo simulation. The simulations were performed using the Geant4 package version 10.07 applying the physical package QGSP\_BERT\_HP and NeutronHPThermalScattering, where the latest is essentially for low-energy neutron interactions with nucleons bound in nuclei. In the simulation, the helium counter tray model was placed in the center of an empty sphere with a diameter of 3 m. Each point of the sphere was an isotropic source of thermal neutrons. The simulated, isotropic neutron flux in the sphere's center can be analytically calculated. Based on the obtained results, the ratio of the simulated counters' counting rate to the simulated neutron flux has been evaluated. The neutron flux at the measurement site was determined from the ratio mentioned above and the measured counting rate.

### 3. Results and Discussion

#### 3.1. Analysis of the Gamma-Ray Spectrum

Based on the in situ measurements of gamma-ray in the EM 'Barbara', detailed analysis of the site was carried out. Figure 3 shows the measured 23 h gamma-ray spectrum in the investigated place. Spectrum counts have been normalized to the day (d), energy (keV), and mass of germanium crystal ( $\text{kg}_{\text{Ge}}$ ). The total number of counts per second (cps) in the collected spectrum for the energy range of 7–3150 keV is  $350.00 \pm 0.05$ . This value is two times lower compared to similar measurements made at the Reiche Zeche mine in Germany at a depth of 150 m in gneiss (702.53 cps) [13] and the Pyhäsalmi mine in Callio Lab in Finland at a depth of 1436 m in sulfide (683.52 cps) [9].

Table 1 lists the effective dose rate and the total apparent activity in the measuring point for all identified radioisotopes in the in situ gamma-ray spectrum.

The gamma-ray flux determined based on in situ measurements in the chamber excavated in sandstone of the EM 'Barbara' is  $17.6 \pm 1.9 \text{ cm}^{-2}\text{s}^{-1}$ , while the effective dose rate is  $0.200 \pm 0.029 \text{ } \mu\text{Sv/h}$ . The most significant contributions to the effective dose rate are potassium  $^{40}\text{K}$  radioisotope (46.9%), bismuth  $^{214}\text{Bi}$  radioisotope (25.1%) from the uranium series, and thallium  $^{208}\text{Tl}$  and actinium  $^{228}\text{Ac}$  radioisotopes from the thorium series (15.2% and 6.6%, respectively). For comparison, the average gamma dose rate density in Katowice (Poland) for ground measurement is  $0.088 \text{ } \mu\text{Sv/h}$  [14]. The effective dose rate estimated in this study in a shallow location (122 m w.e.) in an unshielded chamber excavated in sandstone is 1.3 times higher than in Callio Lab at a depth of 4000 m w.e. within the volcanogenic massive sulfide deposit, 25 times higher than in the Polkowice-Sieroszowice

mine in the anhydrite layer at a depth of 2941.8 m w.e., and 5.7 times higher than in the Reiche Zeche mine in a chamber covered with gneiss (Alte Elisabeth shaft) at a depth of 410 m w.e. On the other hand, the gamma-ray flux is about seven times higher than in another shallow location in the Reiche Zeche mine (410 m w.e.) and about 28 times higher than in the deep location Polkowice-Sieroszowice mine (2941.8 m w.e.). Compared to the leading deep European underground laboratories, the gamma-ray flux in the Experimental Barbara mine is about 140 times higher than in Boulby in Great Britain (0.128 cm<sup>-2</sup>s<sup>-1</sup> at 2800 m w.e.) [15] and 120 times higher than in Gran Sasso in Italy in the parent rock-dolomite limestone (0.151 cm<sup>-2</sup>s<sup>-1</sup> at 3200 m w.e.) [16].

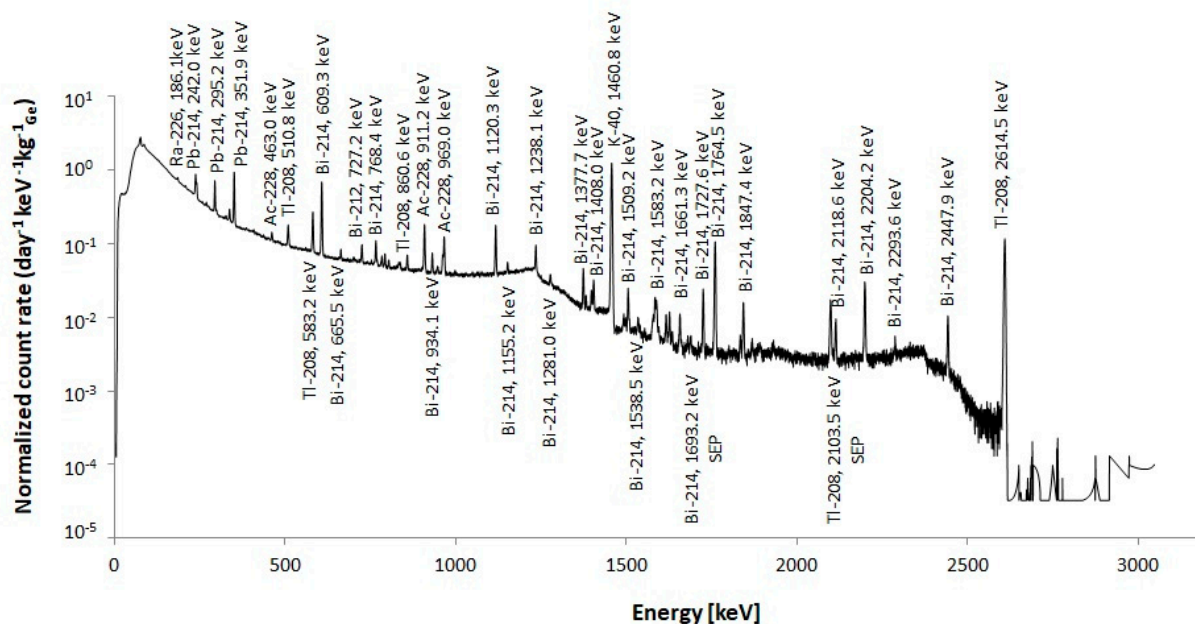


Figure 3. Gamma-ray spectrum registered in situ in blind chamber excavated in sandstone, in the EM ‘Barbara’, using HPGe detector, with main visible peaks.

Table 1. Effective dose rate (EDR), with the relative contribution (%) to each radionuclide to EDR, and total apparent activity associated with each source of photon radiation recognized at the spectrum registered in situ.

Decay Chain	Nuclide	Apparent [Bq/cm <sup>2</sup> ]	Δ [Bq/cm <sup>2</sup> ]	EDR [pSv/s]	Δ [pSv/s]	% to EDR
Uranium	<sup>234</sup> Th	3.36	0.59	0.025	0.004	0.05
	<sup>234m</sup> Pa	1.23	0.40	0.032	0.011	0.06
	<sup>226</sup> Ra	1.89	0.42	0.036	0.006	0.06
	<sup>214</sup> Bi	3.26	0.38	13.97	2.07	25.13
	<sup>214</sup> Pb	2.55	0.51	1.85	0.27	3.32
	<sup>210</sup> Pb	2.45	0.34	0.018	0.003	0.03
Thorium	<sup>228</sup> Ac	1.45	0.40	3.66	0.54	6.60
	<sup>208</sup> Tl	0.63	0.18	8.43	1.23	15.16
	<sup>212</sup> Pb	1.12	0.21	0.342	0.049	0.61
	<sup>212</sup> Bi	1.92	0.23	0.571	0.085	1.03
None	<sup>40</sup> K	51.63	5.10	26.06	3.70	46.88
	<sup>239</sup> Pu	19.00	5.06	0.011	0.002	0.02
	X-rays			0.343	0.049	0.62
	Annihilation			0.242	0.035	0.44



### 3.2. The Ratio of K-40/Bi-214

One indicator of the level of naturally occurring gamma radiation in underground locations is the counting rate under the peak of the  $^{40}\text{K}$  potassium radioisotope (1460.8 keV) in relation to the count rate under the peak of bismuth radioisotope  $^{214}\text{Bi}$  (1764.5 keV). This ratio is determined due to the leading contribution of the  $^{214}\text{Bi}$  radioisotope from the uranium series in the gamma radiation spectrum as a derivative of radon and the ubiquitous  $^{40}\text{K}$  potassium radioisotope in the environment. This parameter also determines the production of radon in rocks and the transport of radon through ventilation ducts. For the tested location in this work (excavation chamber), the  $^{40}\text{K}/^{214}\text{Bi}$  counting rate ratio is 12.3, which is typical for shallow underground localizations (several tens of meters) [10]. This coefficient was also measured in other works. For comparison, the research performed in the shallow (150 m) Reiche Zeche mine in the Alte Elisabeth shaft, in a bare rock cave, the value of the  $^{40}\text{K}/^{214}\text{Bi}$  ratio was 9.22 [13]. However, for deeper locations, the value of this coefficient decreases. For the Polkowice-Sierszowice mine, the coefficient equals 3.8 for a depth of 1014.4 m, for Modane 2.27 [17] for a depth of 1200 m, and for Gran Sasso 1.56 [16] for a depth of 1400 m.

### 3.3. Radon Concentration in Air

The measurement of radon  $^{222}\text{Rn}$  in the air was carried out from 10 to 11 September 2020. After closing the door to the measurement chamber and cutting off the airflow to the chamber, an increase in radon concentration was observed. The concentration of  $^{222}\text{Rn}$  varied from  $42 \pm 26 \text{ Bq/m}^3$  to  $4040 \pm 150 \text{ Bq/m}^3$ . In addition, a high  $^{222}\text{Rn}$  concentration equal to  $805.1 \pm 10.4 \text{ Bq/m}^3$  was observed in the Reiche Zeche mine of Freiberg, Germany, at the higher depth (150 m) within the gneiss formation [13]. For comparison, the measurements of  $^{222}\text{Rn}$  concentrations in 200 underground tourist routes in Poland have shown values over  $20\,000 \text{ Bq/m}^3$  with the arithmetic mean of  $1610 \text{ Bq/m}^3$  [18]. It is well known that exposure to a high radon concentration may cause lung cancer [19]. The radon concentration in underground laboratories depended on several factors, including soil/surrounding rocks characteristics, ventilation facilities, meteorological conditions, temperature, humidity, etc. [20]. The radon background is one of the most critical parameters for ultra-low background and rare-event physical experiments in underground laboratories [20]. For example, LSM Modane provides a low-radon clean room to achieve radon concentration lower than  $100 \text{ mBq/m}^3$  for radiobiology experiments and nanoelectronics fabrication [21].

### 3.4. Radioactivity Content in Rocks

The activity concentration of the  $^{40}\text{K}$  isotope varies in the range from  $434 \pm 7 \text{ Bq/kg}$  to  $609 \pm 10 \text{ Bq/kg}$  with the arithmetic mean and the median equal to  $517 \text{ Bq/kg}$  and  $527 \text{ Bq/kg}$ , respectively. The  $^{226}\text{Ra}$  concentration ranged from  $8.1 \pm 0.4 \text{ Bq/kg}$  to  $54.4 \pm 1.8 \text{ Bq/kg}$  (mean:  $18.3 \text{ Bq/kg}$ , median:  $13.7 \text{ Bq/kg}$ ). The values of  $^{228}\text{Ra}$  concentrations ranged from  $7.0 \pm 0.3 \text{ Bq/kg}$  to  $31.5 \pm 0.7 \text{ Bq/kg}$  with the mean equal to  $15.6 \text{ Bq/kg}$  and the median equal to  $12.5 \text{ Bq/kg}$ . The analyzed rock samples exhibited the variability of the  $^{226,228}\text{Ra}$  concentrations. The worldwide average activity concentrations of  $^{226}\text{Ra}$ ,  $^{232}\text{Th}$ , and  $^{40}\text{K}$  in the earth's crust are equal to  $40 \text{ Bq/kg}$ ,  $40 \text{ Bq/kg}$ , and  $400 \text{ Bq/kg}$ , respectively [22]. Hence, the median values of  $^{226,228}\text{Ra}$  concentrations were lower than the above-mentioned worldwide average  $^{226,228}\text{Ra}$  activity concentrations in the earth's crust. For comparison,  $^{226,228}\text{Ra}$  concentrations were higher than values observed in the Polkowice-Sierszowice mine in Poland at a depth of 1014.4 m within the anhydrite layer [10]. The  $^{226,228}\text{Ra}$  concentrations obtained in the present study were in range of values obtained at Lab 2 of Callio Lab, Pyhäsalmi mine in Finland at a depth of 1436 m [9]. The concentrations of  $^{238}\text{U}$  isotope in the analyzed sandstone samples vary in the range from  $10.4 \pm 0.8 \text{ Bq/kg}$  to  $21.6 \pm 1.0 \text{ Bq/kg}$  (mean:  $14.8 \text{ Bq/kg}$ , median:  $15.0 \text{ Bq/kg}$ ) and for  $^{234}\text{U}$  isotope from  $10.4 \pm 0.8$  to  $22.2 \pm 1.1 \text{ Bq/kg}$  (mean and median:  $15.1 \text{ Bq/kg}$ ). Based on the  $^{238}\text{U}$  concentration, the calculated uranium content was in the range  $0.84 \pm 0.06$  to  $1.75 \pm 0.08 \text{ ppm}$ . The analyzed samples exhibited a radioactive equilibrium between  $^{234}\text{U}$

and  $^{238}\text{U}$  isotopes (the mean and the median of  $^{234}\text{U}/^{238}\text{U}$  activity ratio was equal to 1.0). The  $^{226}\text{Ra}/^{238}\text{U}$  activity ratio varied from  $0.82 \pm 0.06$  to  $1.16 \pm 0.07$  with the mean and the median equal to 1.0. This result also suggests a radioactive equilibrium between the  $^{238}\text{U}$  isotope and daughter isotope  $^{226}\text{Ra}$ . Previous studies [23] of  $^{226}\text{Ra}$  concentrations in rocks collected in the southern part of the Lower Silesia also showed low values of this isotope in sandstones (3.0–33 Bq/kg, mean: 12.8 Bq/kg). In addition, low U, Th mass values,  $^{226,228}\text{Ra}$ , and  $^{40}\text{K}$  concentrations were observed in sandstone samples collected in waste from coal combustion on a heap mine belonging to the Polish Mining Group [24].

### 3.5. Qualitative Neutron Activation Analysis

One of the samples taken from the rock was subjected to neutron activation with a source of californium ( $^{252}\text{Cf}$ ). The sample was activated for one month. Immediately after activation, gamma measurements were made with the HPGe detector described in Section 2.3. These measurements were carried out to investigate the effect of neutrons on the production of radionuclides in the studied location. The higher intensity of the neutron flux in the underground location could affect the gamma-ray spectrum and increase the radiation hazard level at this location.

Gamma-ray measurements were taken in several cycles (a few minutes of measurements immediately after activation and several hours and several days) to record the short-lived and long-lived radioisotopes produced in the  $(n,\gamma)$  reaction.

Several radioactive isotopes resulting from the reaction  $(n,\gamma)$  with gamma probability emission intensity were identified in the recorded gamma-ray spectra of the activated sample. They were:  $^{56}\text{Mn}$  (846.8 keV (98.9%)),  $^{46}\text{Sc}$  (889.3 keV (100%), 1120.2 keV (100%)),  $^{24}\text{Na}$  (1368.6 keV (100%)),  $^{42}\text{K}$  (1524.7 keV (18%)),  $^{140}\text{La}$  (487.0 keV (45.5%), 1596.2 keV (95.4%)) [25]. The identified radioisotopes in the gamma-ray spectrum suggest that they come from activated admixtures in sandstone.

### 3.6. Neutron Flux Results

Data were collected for approximately 2 weeks (11–23 September 2020). Periods with a large level of noise were excluded from the analysis. Therefore, the lifetime of data collection by the ZDAJ counters was about 12 days. On the other hand, the Centronic counters collected good quality data for 27 h only, which was probably due to a failure of the HV power supply. In addition, data from one of the Centronic counters were not suitable for analysis. Equipment problems were probably the result of a large increase in humidity in the measurements room.

For the individual counter, the neutron counting rate, i.e., counting rate for signals with an amplitude from the area of the neutron peak or smaller (“peak and tail”) was determined by creating histograms of the number of counts in a given time and fitting them with Gaussian distributions. By averaging the results for counters of the same type, one can get a counting rate of  $16.6 \pm 2.8$  for Centronic and  $6.8 \pm 1.2$  for ZDAJ (per counter per hour). The result for ZDAJ counters is approximately two times lower than that for Centronic counters, since the surface area of ZDAJ counters is about twice smaller than that of Centronic counters. A similar analysis method was used to determine the counting rate of signals with an amplitude greater than the neutron peak, i.e., signals from alpha particles emitted from the elements of the counter itself. This radioactivity is known from previous laboratory measurements and should not depend on the measurement conditions, so it can be considered a test source. After taking into account the measured energy range, the average rate of counts was  $6 \pm 2$  for ZDAJ and  $14 \pm 2$  for Centronic per counter per hour, which is close to expected ( $3.2 \text{ h}^{-1}$  and  $16.2 \text{ h}^{-1}$  respectively).

After comparing the neutron counting rate with the Monte Carlo simulations (described above), the neutron flux can be calculated, and for ZDAJ counters, it is equal to  $(8.2 \pm 1.5) \times 10^{-6} \text{ cm}^{-2}\text{s}^{-1}$  and for Centronic:  $(9.1 \pm 1.5) \times 10^{-6} \text{ cm}^{-2}\text{s}^{-1}$ . As both results are consistent within the limits of the errors, it makes sense to use the average of the neutron flux determined for individual counters, and it is equal to  $(8.6 \pm 1.1) \times 10^{-6} \text{ cm}^{-2}\text{s}^{-1}$ . This

result can be compared to our previous measurements obtained with a similar setup and method. The results have been summarized in Table 2 (the previous version of this table was published in our previous work [10]).

**Table 2.** Comparison of thermal neutron flux measurement in different European underground locations (complemented based on [10]).

Location	Flux of Thermal Neutrons ( $\times 10^{-6} \text{ cm}^{-2} \text{ s}^{-1}$ )
Barbara, (Poland)	$8.6 \pm 1.1$ (this work)
Polkowice-Sieroszowice, (Poland)	$2.0 \pm 0.2$ [10]
Gran Sasso, (Italy)	$0.56 \pm 0.22$ [26]
Slanic Prahova, (Romania)	$0.12 \pm 0.05$ [26]
Freiberg, (Germany)	$3.12 \pm 0.10$ [13]
Pyhäsalmi; Lab 2, (Finland)	$17.30 \pm 0.10$ [9]

The neutron flux in the EM ‘Barbara’ turns out to be relatively high, the highest except at Lab 2 in Pyhäsalmi, where the radiation source was probably the blast furnace slag used as filler in the concrete casing of the chamber. The decision regarding the source of the neutrons in the EM ‘Barbara’ mine is not clear and would require additional research.

#### 4. Conclusions

The measurements performed in the chamber located at the depth 46 m (122 m w.e.) in the sandstone layer showed a low content of analyzed radionuclides. The sandstone layer shallowly located under the surface in the Upper Silesia region shows a relatively high content of potassium ( $^{40}\text{K}$  is responsible for nearly 50% of the effective dose rate in the studied location). The absence of summation peaks on the registered in situ spectrum suggests a relatively lower content of uranium daughters than in other shallow locations studied previously by us, e.g., Reiche Zeche mine [13]. However, the  $^{40}\text{K}/^{214}\text{Bi}$  ratio in both these locations is typical for shallow underground sites.

Assuming 2000 working hours per year, an effective dose rate of  $0.2 \mu\text{Sv/h}$  determined here, amounts of  $0.4 \text{ mSv}$  do not increase the gamma-ray radiation hazard for mineworkers compared with the total population.

The high radon concentration was associated with the closing of the utility hole and the shutdown of ventilation. The increased value of the gamma-ray flux may partly come from gamma radon daughters. Hence, an important parameter related to the activities of the underground laboratory and radiation protection of employees is ventilation, ensuring a low radon level.

The presented results of thermal neutron flux measurements are relatively high compared to other underground locations where similar measurements were performed. In order to make a credible hypothesis why this is so, it would be crucial to identify the source of the measured neutrons. In general, the neutrons in the underground environment come from the fission of uranium present in rocks, from reactions of the  $(\alpha, n)$  type, where alpha particles from the decay of radioactive elements interact with the nuclei of light elements, causing emissions of neutrons, and also from the interaction of cosmic rays muons. The neutrons emitted by these processes differ in their energy spectrum, so in principle, these processes could be distinguished by measuring energy. However, the problem is that the neutrons born inside the rocks “thermalize” before they reach the detector; i.e., they lose energy on elastic scattering on the atomic nuclei of the matter being penetrated. This process effectively distorts the energy spectrum of neutrons. The thermalization process depends not only on the chemical composition of the rocks but also on their humidity (because hydrogen is an excellent thermalizer, since its mass is similar to a neutron mass). In the present study, helium counters were used, which are the most sensitive to neutrons that have already achieved thermal equilibrium, the so-called “thermal neutrons”. It is a reasonable approach to determine the overall neutron flux at a given location (since each neutron tends to a state of thermal equilibrium) but says nothing about their primary energy.

Therefore, we can only state that the thermal neutron flux is relatively high, as shown in Table 2. A quantitative explanation of the neutrons' origin requires further detailed study in this area.

**Author Contributions:** Conceptualization, A.W.-Ł., K.S., J.K., J.S., K.P.-G. and R.H.; methodology, A.W.-Ł., K.S., J.K., K.P.-G., K.J., J.S., M.K., J.O., P.T., W.M. and M.P.; formal analysis, A.W.-Ł., K.S. and K.J.; investigation, A.W.-Ł., K.S., J.K., K.P.-G., K.J. and M.K.; resources, R.H.; writing—original draft preparation, A.W.-Ł., K.S., K.J., K.P.-G., R.H. and K.F.; writing—review and editing, A.W.-Ł., K.S., J.K. and K.F.; visualization, J.K.; supervision, J.K. All authors have read and agreed to the published version of the manuscript.

**Funding:** This research was funded by: Interreg Baltic Sea Region, grant number: #R037 Baltic Sea Underground Innovation Network (BSUIN) and #X010 Empowering Underground Laboratories Network Usage (EUL); the Research Excellence Initiative of the University of Silesia in Katowice; and the Polish Ministry of Science and Higher Education (grant No. 3988/INTERREG BSR/2018/2).

**Institutional Review Board Statement:** Not applicable.

**Informed Consent Statement:** Not applicable.

**Data Availability Statement:** The data presented in this study are available on request from the corresponding author.

**Conflicts of Interest:** The authors declare no conflict of interest.

## References

1. Bettini, A. The world underground scientific facilities. *arXiv* **2007**, arXiv:0712.1051.
2. Bettini, A. The world deep underground laboratories. *Eur. Phys. J. Plus* **2012**, *127*, 114. [[CrossRef](#)]
3. Niese, S.; Koehler, M.; Gleisberg, B. Low-level counting techniques in the underground laboratory “Felsenkeller” in Dresden. *J. Radioanal. Nucl. Chem.* **1998**, *233*, 167–172. [[CrossRef](#)]
4. Oeschger, H.; Beer, J.; Loosli, H.H.; Schotterer, U. Low-level counting systems in deep underground laboratories. In Proceedings of the International Symposium on Methods of Low-Level Counting and Spectrometry, Berlin, Germany, 6–10 April 1981; pp. 459–474, IAEA-SM 252/13.
5. Kalin, R.; Long, A. Radiocarbon dating with the quantulus in an underground counting laboratory; performance and background sources. *Radiocarbon* **1989**, *31*, 359–367. [[CrossRef](#)]
6. Lindstrom, R.M.; Lindstrom, D.J.; Slaback, L.A.; Langland, J.K. A low-background gamma-ray assay laboratory for activation analysis. *Nucl. Instrum. Methods Phys. Res. A* **1990**, *299*, 425–429. [[CrossRef](#)]
7. Heusser, G. Background in Ionizing Radiation Detection—Illustrated by Ge-Spectrometry. In Proceedings of the 3rd International Summer School on Low-Level Measurements of Radioactivity in the Environment Techniques and Applications, Huelva, Spain, 20 September–2 October 1993.
8. Hu, Q.; Weng, J.; Wang, J. Sources of anthropogenic radionuclides in the environment: A review. *J. Radioanal. Nucl. Chem.* **2010**, *101*, 426–437. [[CrossRef](#)] [[PubMed](#)]
9. Polaczek-Grelak, K.; Walencik-Łata, A.; Szkliniarz, K.; Kisiel, J.; Jędrzejczak, K.; Szabelski, J.; Kasztelan, M.; Joutsenvaara, J.; Puputti, H.J.; Holma, M.; et al. Natural background radiation at Lab 2 of Callio Lab, Pyhäsalmi mine in Finland. *Nucl. Instrum. Methods Phys. Res. A* **2020**, *969*, 164015. [[CrossRef](#)]
10. Szkliniarz, K.; Walencik-Łata, A.; Kisiel, J.; Polaczek-Grelak, K.; Jędrzejczak, K.; Kasztelan, M.; Szabelski, J.; Orzechowski, J.; Tokarski, P.; Marszał, W.; et al. Characteristics of Natural Background Radiation in the Polkowice-Sierszowice Mine, Poland. *Energies* **2021**, *14*, 4261. [[CrossRef](#)]
11. ICRP; Petoussi-Henss, N.; Bolch, W.E.; Eckerman, K.F.; Endo, A.; Hertel, H.; Hunt, J.; Pelliccioni, M.; Schlattl, H.; Zankl, M. *Conversion Coefficients for Radiological Protection Quantities for External Radiation Exposures*; Publication 116; Ann. ICRP 40(2–5); ICRP: Stockholm, Sweden, 2010.
12. Walencik-Łata, A.; Smółka-Danielowska, D.  $^{234}\text{U}$ ,  $^{238}\text{U}$ ,  $^{226}\text{Ra}$ ,  $^{228}\text{Ra}$  and  $^{40}\text{K}$  concentrations in feed coal and its combustion products during technological processes in the Upper Silesian Industrial Region, Poland. *Environ. Pollut.* **2020**, *267*, 115462. [[CrossRef](#)]
13. Polaczek-Grelak, K.; Walencik-Łata, A.; Szkliniarz, K.; Kisiel, J.; Jędrzejczak, K.; Szabelski, J.; Mueller, T.; Schreiter, F.; Djakonow, A.; Lewandowski, R.; et al. Characterization of the radiation environment at TU Bergakademie in Freiberg, Saxony, Germany. *Nucl. Instrum. Methods Phys. Res. A* **2019**, *946*, 162652. [[CrossRef](#)]
14. National Atomic Energy Agency. Available online: <https://www.gov.pl/web/paa/sytuacja-radiacyjna> (accessed on 11 November 2021).
15. Malczewski, D.; Kisiel, J.; Dorda, J. Gamma background measurements in the Boulby Underground Laboratory. *J. Radioanal. Nucl. Chem.* **2013**, *298*, 1483–1489. [[CrossRef](#)]

16. Malczewski, D.; Kisiel, J.; Dorda, J. Gamma background measurements in the Gran Sasso National Laboratory. *J. Radioanal. Nucl. Chem.* **2013**, *295*, 749–754. [[CrossRef](#)] [[PubMed](#)]
17. Malczewski, D.; Kisiel, J.; Dorda, J. Gamma background measurements in the Laboratoire Souterrain de Modane. *J. Radioanal. Nucl. Chem.* **2012**, *292*, 751–756. [[CrossRef](#)]
18. Olszewski, J.; Zmysłony, M.; Wrzesień, M.; Walczak, K. The occurrence of radon in Polish underground tourist routes. *Med. Pr.* **2015**, *66*, 557–563. [[CrossRef](#)]
19. Kim, S.-H.; Hwang, W.J.; Cho, J.-S.; Kang, D.R. Attributable risk of lung cancer deaths due to indoor radon exposure. *Ann. Occup. Environ. Med.* **2016**, *28*, 8. [[CrossRef](#)]
20. Liu, C.; Ma, H.; Zeng, Z.; Cheng, J.; Li, J.; Zhang, H. Measurements of Radon Concentrations Using CR-39 Detectors in China JinPing Underground Laboratory (2015-2016). *arXiv* **2018**, arXiv:1806.06567.
21. Štekl, I.; Hůlka, J.; Mamedov, F.; Fojtík, P.; Čermáková, E.; Jílek, K.; Havelka, M.; Hodák, R.; Hýža, M. Low Radon Cleanroom for Underground Laboratories. *Public Health Front.* **2021**, *8*, 1086. [[CrossRef](#)] [[PubMed](#)]
22. European Commission. *Radiological Protection Principles Concerning the Natural Radioactivity of Building Materials*; Radiation Protection; European Commission, Directorate-General, Environment, Nuclear Safety and Civil Protection: Luxembourg, Belgium, 1999; p. 112.
23. Przylibski, T.A. Concentration of  $^{226}\text{Ra}$  in rocks of the southern part of Lower Silesia (SW Poland). *J. Environ. Radioact.* **2004**, *75*, 171–191. [[CrossRef](#)] [[PubMed](#)]
24. Smółka-Danielowska, D.; Walencik-Lata, A. The Occurrence of Selected Radionuclides and Rare Earth Elements in Waste at the Mine Heap from the Polish Mining Group. *Minerals* **2021**, *11*, 504. [[CrossRef](#)]
25. Firestone, R.B.; Shirley, V.S. *Tables of Isotopes*; John Wiley & Sons Inc: Hoboken, NJ, USA, 1996.
26. Dębicki, Z.; Jędrzejczak, K.; Kaczmarczyk, J.; Kasztelan, M.; Lewandowski, R.; Orzechowski, J.; Szabelski, J.; Szeptycka, M.; Tokarski, P. Neutron flux measurements in the Gran Sasso national laboratory and in the Slanic Prahova Salt Mine. *Nucl. Instrum. Methods Phys. Res. A* **2018**, *910*, 133–138. [[CrossRef](#)]